5'-Triphosphate-Dependent Activation of PKR by RNAs with Short Stem-Loops
Subba Rao Nallagatla, *et al.*
Science **318**, 1455 (2007);
DOI: 10.1126/science.1147347

Bildung und Forschung, the IZKF Leipzig (H.R., C.S., and T.S.), and the Studienstiftung des Deutschen Volkes (C.S.) for financial support. The excavation at El Sidrón is supported by the Autonomous Government of Asturias. The study of the Monti Lessini Neanderthal is framed into a research project on human fossil remains at the Verona Natural History Museum. The Neanderthal *mc1r* sequence has been deposited at GenBank, accession number EU204643.

Supporting Online Material
www.sciencemag.org/cgi/content/full/1147417/DC1
Materials and Methods
Figs. S1 to S5
Tables S1 to S4
References

5 July 2007; accepted 12 October 2007
Published online 25 October 2007;
10.1126/science.1147417
Include this information when citing this paper.

5′-Triphosphate–Dependent Activation of PKR by RNAs with Short Stem-Loops

Subba Rao Nallagatla,[1]* Jungwook Hwang,[2]* Rebecca Toroney,[1] Xiaofeng Zheng,[1,3] Craig E. Cameron,[2,4]† Philip C. Bevilacqua[1]†

Molecular patterns in pathogenic RNAs can be recognized by the innate immune system, and a component of this response is the interferon-induced enzyme RNA-activated protein kinase (PKR). The major activators of PKR have been proposed to be long double-stranded RNAs. We report that RNAs with very limited secondary structures activate PKR in a 5′-triphosphate–dependent fashion in vitro and in vivo. Activation of PKR by 5′-triphosphate RNA is independent of RIG-I and is enhanced by treatment with type 1 interferon (IFN-α). Surveillance of molecular features at the 5′ end of transcripts by PKR presents a means of allowing pathogenic RNA to be distinguished from self-RNA. The evidence presented here suggests that this form of RNA-based discrimination may be a critical step in mounting an early immune response.

The innate immune response offers the host early protection from foreign organisms and viruses (*1*). As part of this response, the double-stranded RNA (dsRNA)–activated protein kinase (PKR) becomes activated through autophosphorylation in the presence of viral RNA (*2*). Subsequently, PKR phosphorylates eukaryotic initiation factor 2α (eIF2α), which inhibits translation initiation, thus preventing pathogen replication (*2*).

PKR can be both activated and inhibited through its interaction with RNA, which is mediated by dsRNA-binding motifs (dsRBMs) (Fig. 1A) that also exist in other diverse proteins, including RNA-specific adenosine deaminases (ADARs), Dicer, and ribonuclease III (*3*). This interaction with dsRNA is sequence-independent (*4*, *5*), and although at least 16 base pairs (bp) of dsRNA are required for inhibition of PKR, 33 bp are needed for activation (*4*, *6*). We have previously shown that short dsRNAs with single-stranded tails (ss-dsRNAs) activate PKR, with the length of the tail providing a critical determinant (*6*). This motif has an imperfect stem of 16 bp and is flanked by single-stranded tails (Fig. 1B), and because it was prepared by transcription, it contains a 5′-triphosphate (*7*). This raises the question of what features of the tail might be important in activating PKR.

In our initial experiments, we observed that a 79-bp perfectly dsRNA (dsRNA-79) led to potent activation of PKR, with an RNA-dependency factor of ~35 (Fig. 1C) (*8*). PKR was also activated by ss-dsRNAs and gave the expected ~10-nucleotide (nt) tail-length dependence (*6*) (Fig. 1C). Maximal activation by ss-dsRNA was as intense as that by dsRNA-79, albeit requiring ~10-fold more RNA. The ss-dsRNA(9,11) (having 5′ and 3′ tails of 9 and 11 nt, respectively) transcript (Fig. 1B) was next treated with calf intestinal phosphatase (CIP) to remove the 5′-triphosphate (fig. S1), leading to abrogation of activation even at higher concentrations (Fig. 1C). Furthermore, chemically synthesized ss-dsRNA(9,11) having a 5′ hydroxyl (fig. S2) also failed to activate PKR. The presence of the 5′-triphosphate led to 100-fold higher PKR activation than occurred in its absence (fig. S2) (*8*). A mixture of CIP-treated and untreated transcripts showed full activation of PKR (fig. S3), indicating that the reason why CIP-treated RNAs do not activate PKR is not because CIP treatment renders PKR incapable of activation.

To test whether the presence of 5′-triphosphate also affects the ability of long dsRNAs to activate PKR, top and bottom strands of dsRNA-79 were CIP-treated and annealed (fig. S4). Unlike ss-dsRNA, CIP-treated as well as untreated dsRNA could activate PKR, with a standard bell-shaped dependence on RNA concentration (fig. S4D) (*6*). Thus, long dsRNA does not require 5′-triphosphate, suggesting that the contribution of this motif to PKR activation is dependent on RNA structure.

Given that ss-dsRNAs have functionally important non–base-paired elements (*6*), we next tested activation by the single strands of dsRNA-79, which also have secondary structure (fig. S4, A and B). CIP-treated ssRNA-79TS (TS, top

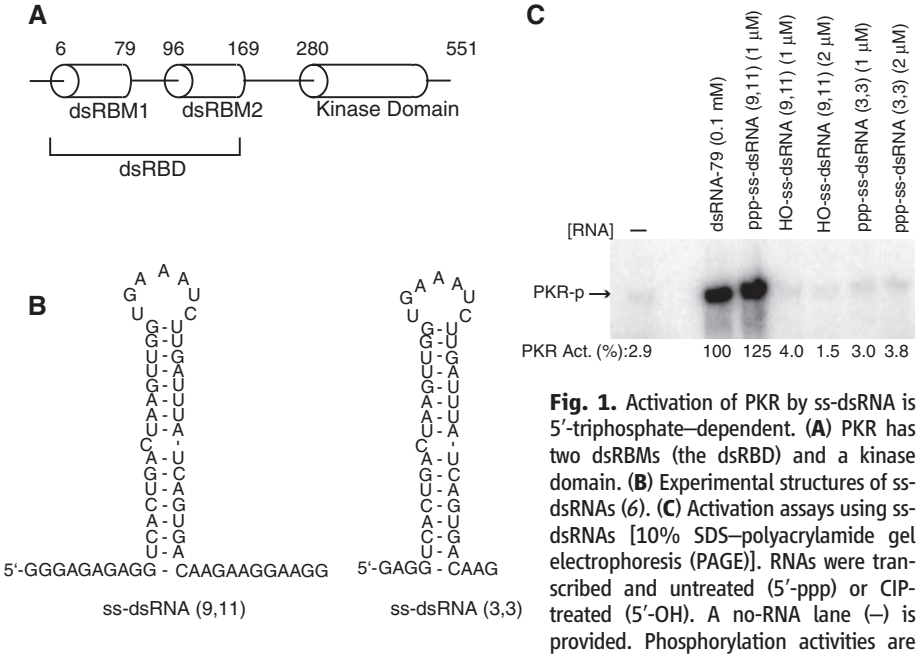

Fig. 1. Activation of PKR by ss-dsRNA is 5′-triphosphate–dependent. (**A**) PKR has two dsRBMs (the dsRBD) and a kinase domain. (**B**) Experimental structures of ss-dsRNAs (*6*). (**C**) Activation assays using ss-dsRNAs [10% SDS–polyacrylamide gel electrophoresis (PAGE)]. RNAs were transcribed and untreated (5′-ppp) or CIP-treated (5′-OH). A no-RNA lane (—) is provided. Phosphorylation activities are normalized to 0.1 μM dsRNA-79 (no CIP).

[1]Department of Chemistry, Pennsylvania State University, University Park, PA 16802, USA. [2]Integrative Biosciences, Pennsylvania State University, University Park, PA 16802, USA. [3]Department of Biochemistry and Molecular Biology, Life Sciences College, Peking University, Beijing 100871, China. [4]Department of Biochemistry and Molecular Biology, Pennsylvania State University, University Park, PA 16802, USA.

*These authors contributed equally to this work.
†To whom correspondence should be addressed. E-mail: pcb@chem.psu.edu (P.C.B.); cec9@psu.edu (C.E.C.)

strand) and ssRNA-79BS (BS, bottom strand) transcripts (*8*) were poor activators, whereas untreated transcripts activated PKR at levels similar to those produced by dsRNA-79 (fig. S4, E and F), with a measurable 5′-triphosphate dependence. The experiments thus far suggest that triphosphate makes the greatest contribution when the 5′ end is unstructured. To examine this further, 47- and 110-nt transcripts with minimal secondary structure were prepared (fig. S5), and despite having only a small number of short stem-loops, both transcripts activated PKR at levels close to those produced by dsRNA-79 (fig. S4, G and H). CIP treatment greatly reduced activation, confirming dependence on 5′-triphosphate.

Many viral and bacterial RNAs possess 5′-triphosphates (*9*, *10*), whereas most cellular transcripts have a 7-methyl-guanosine (7mG) cap or a 5′-monophosphate. Thus, it is possible that PKR uses the 5′ end of mRNA as part of a quality control mechanism (*11*). 5′-monophosphate or 5′-hydroxyl termini, prepared by chemical synthesis of ssRNA-47, were at least 50-fold less effective than a 5′-triphosphate terminus, yielding no detectable activation (*8*) [Fig. 2 and supporting online material (SOM) text]. Transcripts primed with a 7mG cap or guanosine diphosphate (GDP) also failed to induce measurable PKR activation (Fig. 2, B to D). Parallel experiments on ssRNA-110 gave similar results (figs. S4G and S6), indicating that longer transcripts also have a dependence on 5′-triphosphate for activation of PKR.

Short 5′-triphosphate double-stranded small interfering RNAs, which induce an interferon response (*12*), as well as related short ssRNAs, failed to activate PKR (fig. S7 and SOM text). This suggested a minimal length of ssRNA required for activation, which we determined to be ~47 nt (fig. S8). In addition, a short (5-bp) stem-loop enhanced the magnitude of the response as well as the dependence on triphosphate (figs. S9 and S10). We also observed that the optimal positioning of the stem-loop in otherwise unstructured ssRNA was 21 to 46 nt from the 5′ end (figs. S9 and S10). One possible reason for this is that short stem-loops assist PKR binding, an idea that is supported by data on a dsRNA-binding domain (dsRBD) binding to 20-bp dsRNA that is consistent with a site size of 6 to 7 bp per dsRBD (*13*). As for other support, RNA/PKR binding assays revealed a correlation between RNA binding and kinase activation (fig. S8, B and C).

One of the biological substrates of PKR is eIF2α, the function of which in translation initiation is inhibited upon phosphorylation of Ser^{51} (*2*). Upon activation by 5′-triphosphate ssRNA, PKR efficiently phosphorylated eIF2α (figs. S11 and S12 and SOM text), with each activated PKR molecule phosphorylating more than 100 eIF2α molecules with a PKR:eIF2α stoichiometry of 1:1. These results are consistent with a recent crystal structure, which showed each monomer in a PKR dimer interacting with an eIF2α protein (*14*).

To explore the biological relevance of our findings thus far, three cell lines were selected to test components of the innate immune response: Huh-7, Huh-7.5, and Vero (Fig. 3). All are responsive to interferon (IFN-α) but produce different levels of IFN-α/β in response to RNA virus (Fig. 3A). Transfection of dsRNA-79 into Huh-7 cells induced activation of PKR and increased levels of eIF2α phosphorylation (Fig. 3B, lane 2). Phosphorylated PKR was not observed in mock-transfected cells, although some eIF2α-p was detected (Fig. 3B, lane 1). For the ssRNA, a 110-nt oligomer was selected, which has the same 5′-end requirements as the 47-nt oligomer (Fig. 2 and fig. S6), because longer RNAs possess superior transfection properties. Although 110-nt oligomer ppp-ssRNA (ppp,

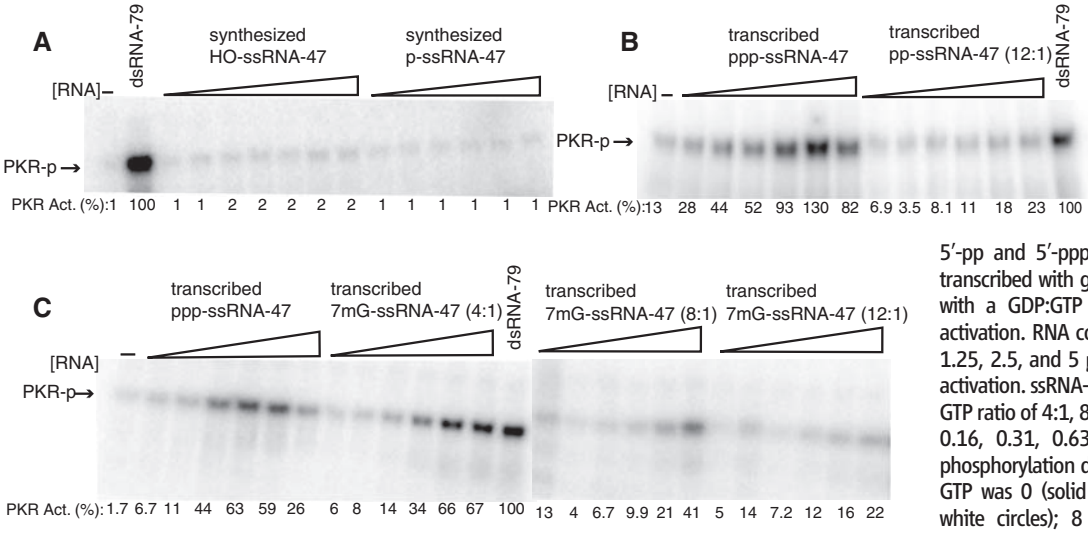

Fig. 2. Activation of PKR by ssRNA is 5′-triphosphate–dependent in vitro. (**A**) Effects of 5′-OH and 5′-p on PKR activation. ssRNA-47 was synthesized with 5′-OH or 5′-p, and concentrations were 0.1, 0.5, 1, 2, 3, 5, and 10 μM (0.1 μM is omitted for 5′-p). (**B**) Effects of 5′-pp and 5′-ppp on PKR activation. ssRNA-47 was transcribed with guanosine triphosphate (GTP) only or with a GDP:GTP ratio of 12:1 and tested for PKR activation. RNA concentrations were 0.16, 0.31, 0.63, 1.25, 2.5, and 5 μM. (**C**) Effect of a 7mG cap on PKR activation. ssRNA-47 was transcribed with a 7mGpppG:GTP ratio of 4:1, 8:1, or 12:1. RNA concentrations were 0.16, 0.31, 0.63, 1.25, 2.5, and 5 μM. (**D**) PKR phosphorylation data from (C). The ratio of 7mGpppG:GTP was 0 (solid line, black circles); 4 (dashed line, white circles); 8 (solid line, black boxes); and 12 (dashed line, white boxes). Phosphorylation activities are normalized to 0.1 μM dsRNA-79 (no CIP).

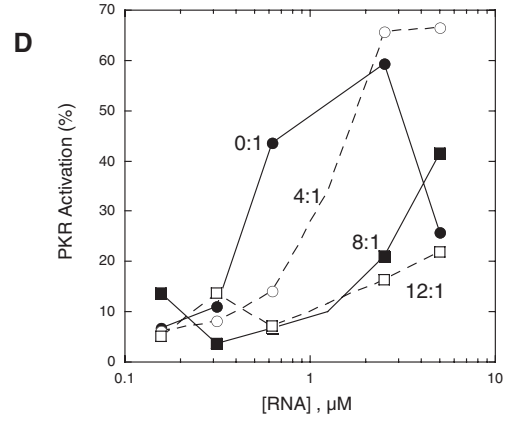

5′-triphosphate) failed to activate PKR to a detectable level, a significant increase in eIF2α-p was nevertheless observed (Fig. 3B, lane 3) relative to mock-transfected cells. The response required the triphosphate, because the CIP-treated ssRNA transcript showed only background levels of eIF2α-p (Fig. 3B, lane 4). These results suggest that ssRNA requires a 5′-triphosphate for PKR-mediated phosphorylation of eIF2α intracellularly.

The helicase and innate immune sensor RIG-I has also recently been shown to be activated by ssRNA with a 5′-triphosphate (*15*, *16*). To determine whether activation of RIG-I contributes to PKR activation by 5′-triphosphate ssRNA, we used the Huh-7.5 subline of Huh-7, which lacks a functional RIG-I signaling pathway (*17*). Activated PKR was not detected in this cell line in response to dsRNA (Fig. 3C, lane 2) or ppp-ssRNA (Fig. 3C, lane 3), although a subtle yet reproducible increase in the amount of eIF2α-p was observed in response to dsRNA treatment (Fig. 3C, lane 2).

It was possible that a requirement for RIG-I for activation of PKR might be due to a need for IFN-α/β production. To test this, Vero cells, which are incapable of producing IFN-α/β, were tested, revealing activation of PKR by dsRNA (Fig. 3D, lane 2) but not ppp-ssRNA (Fig. 3D, lane 3). These data show that activation of PKR by dsRNA is independent of IFN-α/β production. Activation of PKR by ppp-ssRNA may use an alternative mechanism, requiring functional RIG-I signaling and/or IFN-α/β production.

All three cell lines we used are known to respond to IFN-α treatment (Fig. 3A). To further dissect the need for RIG-I signaling from IFN-α/β production, the experiments were repeated in cells treated with IFN-α. In all cell lines, dsRNA activated PKR on the basis of detection of both PKR-p and eIF2α-p (Fig. 3, B to D, lane 6). These experiments demonstrate that RIG-I signaling is not required for PKR activation by dsRNA. Likewise, ppp-ssRNA activated PKR in all cell lines treated with IFN-α, with both PKR-p and eIF2α-p being detected (Fig. 3, B to D, lane 7), indicating that RIG-I signaling is not required for PKR activation by ppp-ssRNA either. CIP-treated ssRNA did not produce significant levels of PKR-p, although this RNA led to some increase in eIF2α-p in Huh-7 cells (Fig. 3, B to D, lane 8), which is probably due to residual triphosphate (*8*). We conclude that ssRNA activates PKR in a 5′-triphosphate–dependent fashion in cells.

The data thus far are consistent with the existence of a "primed" form of cellular PKR, which is induced by IFN-α treatment and required for effective activation of PKR by ppp-ssRNA. This conclusion is based on the observation that PKR activation by 5′-triphosphate ssRNA shows a strict dependency on IFN (Fig. 3, B to D, lanes 3 and 7) whereas PKR activation by dsRNA does not (Fig. 3, B and D, lanes 2 and 6). ppp-ssRNA is more potent than dsRNA in activating PKR in IFN-α–treated Huh-7 cells (Fig. 3B, lanes 6 and 7). Alternatively, it is possible that a higher PKR concentration, which is stimulated by IFN, is required for ppp-ssRNA–mediated activation of PKR.

For ssRNA-110, only a transcript with a 5′-triphosphate was capable of activating PKR intracellularly, and it also showed the greatest potency of activation of eIF2α (Fig. 3E). [The low levels of activation of eIF2α that were present for 5′-hydroxyl and the 7mG cap may be due to residual triphosphate (*8*).] In agreement with in vitro experiments, activation of PKR by ssRNA-79TS was 5′-triphosphate–dependent whereas activation by dsRNA-79 was not (Fig. 3F). Activation by ssRNA-79BS RNA was not 5′-triphosphate–dependent in cells; however, this transcript has a complex secondary structure (fig. S4A), which may facilitate the 5′-triphosphate–independent mode of activation. Indeed, a few RNAs with complex secondary structures are known to activate PKR, including RNA from hepatitis delta virus, the 3′ untranslated region from human alpha-tropomyosin, and various aptamers to PKR's dsRBD (*18*–*20*).

The results presented here reveal that ssRNAs with very limited secondary structures have the ability to activate PKR in a 5′-triphosphate–dependent fashion. These activators differ from classical dsRNA activators. In particular, we have found that activation in a cellular context requires just 5 bp of RNA and is IFN-α–dependent but independent of RIG-I signaling (*15*, *16*). There is evidence that a number of ssRNA viruses use non-dsRNA to activate PKR in vivo (*21*). In particular, influenza virus has a 5′-triphosphorylated single-stranded viral RNA that activates PKR (*22*) and does not produce detectable levels of dsRNA during replication (*16*). It is also notable that several virus families have evolved use of a protein primer that bypasses the presence of a triphosphate at the 5′ end of RNA (*9*), which might represent a mechanism to evade PKR activation. 5′-triphosphate–

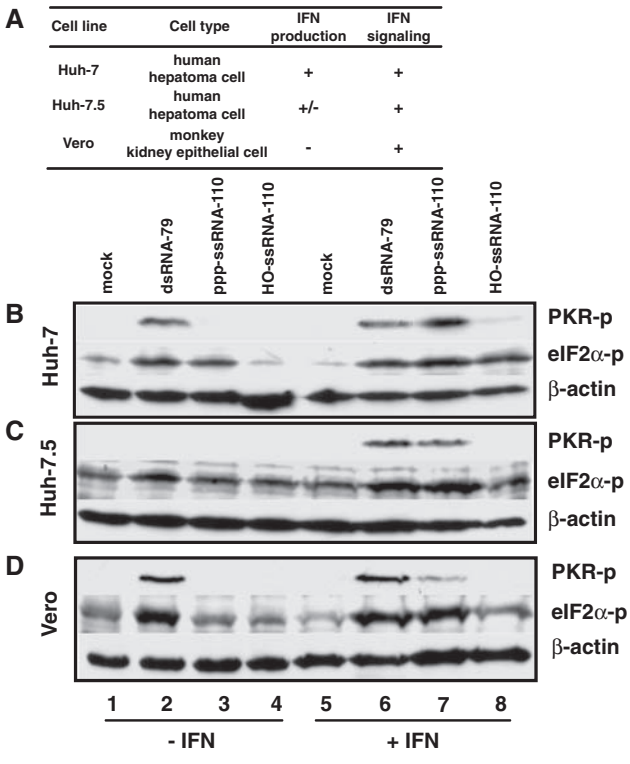

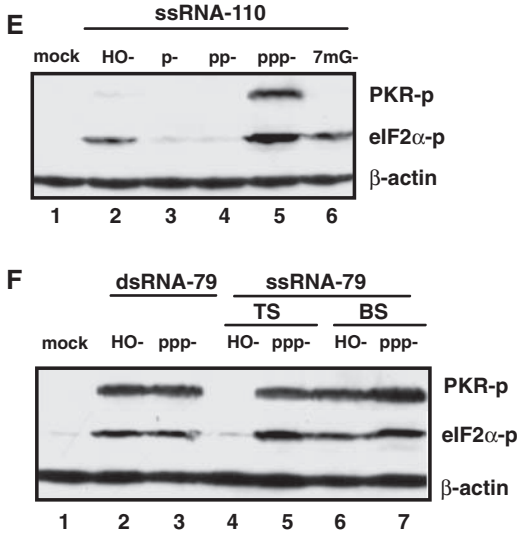

Fig. 3. Activation of PKR by ssRNA is 5′-triphosphate–dependent in vivo. (**A**) Origin of cell line, capacity to produce IFN-α/β, and capacity to signal from the IFN-α/β receptor are indicated. A block of IFN-α/β production in Huh-7.5 cells is observed only if RIG-I signaling is required (*17*). The IFN-α/β gene cluster is deleted in Vero cells (*23*). (**B** to **D**) Cells were plated 24 hours before transfection in the absence (lanes 1 to 4) or presence (lanes 5 to 8) of 1000 units of IFNα per milliliter. Cells were transfected with RNA (2 μg), prepared as for in vitro experiments. Proteins were denatured in SDS buffer and resolved by 10% SDS-PAGE. Phosphorylated PKR (PKR-p), phosphorylated eIF2α (eIF2α-p), and β actin (loading control) were identified by Western blotting. (**E**) Experiments were performed as in (B) using ssRNA-110. The 5′ end was prepared by no treatment (ppp- lane). CIP treatment (HO lane), or priming transcription with a modified guanosine. (**F**) The 5′ ends of dsRNA-79, ssRNA-79TS, and ssRNA-79BS were prepared as in (E). Samples in (E) and (F) were IFN-treated.

dependent activation of PKR by ssRNA may be a major pathway for sensing and responding to viral infection in vivo.

References and Notes

1. G. R. Stark, I. M. Kerr, B. R. Williams, R. H. Silverman, R. D. Schreiber, *Annu. Rev. Biochem.* **67**, 227 (1998).
2. T. E. Dever, A. C. Dar, F. Sicheri, in *Translational Control in Biology and Medicine*, M. B. Mathews, N. Sonenberg, J. W. Hershey, Eds. (Cold Spring Harbor Laboratory Press, Cold Spring Harbor, NY, 2007), pp. 319–344.
3. B. Tian, P. C. Bevilacqua, A. Diegelman-Parente, M. B. Mathews, *Nat. Rev. Mol. Cell Biol.* **5**, 1013 (2004).
4. L. Manche, S. R. Green, C. Schmedt, M. B. Mathews, *Mol. Cell. Biol.* **12**, 5238 (1992).
5. P. C. Bevilacqua, T. R. Cech, *Biochemistry* **35**, 9983 (1996).
6. X. Zheng, P. C. Bevilacqua, *RNA* **10**, 1934 (2004).
7. J. F. Milligan, D. R. Groebe, G. W. Witherell, O. C. Uhlenbeck, *Nucleic Acids Res.* **15**, 8783 (1987).
8. Materials and methods are available as supporting material on *Science* Online.
9. *Fields Virology*, D. Knipe, P. M. Howley, Eds. (Lippincott Williams & Wilkins, Philadelphia, PA, ed. 5, 2007).
10. C. D. Bieger, D. P. Nierlich, *J. Bacteriol.* **171**, 141 (1989).
11. L. E. Maquat, G. G. Carmichael, *Cell* **104**, 173 (2001).
12. D. H. Kim *et al.*, *Nat. Biotechnol.* **22**, 321 (2004).
13. J. W. Ucci, J. L. Cole, *Biophys. Chem.* **108**, 127 (2004).
14. A. C. Dar, T. E. Dever, F. Sicheri, *Cell* **122**, 887 (2005).
15. V. Hornung *et al.*, *Science* **314**, 994 (2006).
16. A. Pichlmair *et al.*, *Science* **314**, 997 (2006).
17. R. Sumpter Jr. *et al.*, *J. Virol.* **79**, 2689 (2005).
18. H. D. Robertson, L. Manche, M. B. Mathews, *J. Virol.* **70**, 5611 (1996).
19. S. Davis, J. C. Watson, *Proc. Natl. Acad. Sci. U.S.A.* **93**, 508 (1996).
20. P. C. Bevilacqua, C. X. George, C. E. Samuel, T. R. Cech, *Biochemistry* **37**, 6303 (1998).
21. J. O. Langland, J. M. Cameron, M. C. Heck, J. K. Jancovich, B. L. Jacobs, *Virus Res.* **119**, 100 (2006).
22. E. Hatada, S. Saito, R. Fukuda, *J. Virol.* **73**, 2425 (1999).
23. J. M. Emeny, M. J. Morgan, *J. Gen. Virol.* **43**, 247 (1979).

24. We thank B. Golden, D. Herschlag, and J. Reese for helpful comments and the following sources for funding: NIH grant GM58709 (P.C.B.) and the Martarano and Berg endowments of the Eberly College of Science (C.E.C.).

Supporting Online Material

www.sciencemag.org/cgi/content/full/318/5855/1455/DC1
Materials and Methods
SOM Text
Figs. S1 to S14
References

3 July 2007; accepted 31 October 2007
10.1126/science.1147347

Direct Observation of Chaperone-Induced Changes in a Protein Folding Pathway

Philipp Bechtluft,[1]* Ruud G. H. van Leeuwen,[2]*† Matthew Tyreman,[2]* Danuta Tomkiewicz,[1] Nico Nouwen,[1]‡ Harald L. Tepper,[2]§ Arnold J. M. Driessen,[1] Sander J. Tans[2]‖

How chaperone interactions affect protein folding pathways is a central problem in biology. With the use of optical tweezers and all-atom molecular dynamics simulations, we studied the effect of chaperone SecB on the folding and unfolding pathways of maltose binding protein (MBP) at the single-molecule level. In the absence of SecB, we find that the MBP polypeptide first collapses into a molten globulelike compacted state and then folds into a stable core structure onto which several α helices are finally wrapped. Interactions with SecB completely prevent stable tertiary contacts in the core structure but have no detectable effect on the folding of the external α helices. It appears that SecB only binds to the extended or molten globulelike structure and retains MBP in this latter state. Thus during MBP translocation, no energy is required to disrupt stable tertiary interactions.

Folding pathways are traditionally studied with isolated proteins, even though the cellular environment often presents interactions with other molecules during the folding process. For instance, interactions with chaperones are often crucial to guide folding, to prevent aggregation, and to facilitate protein translocation across membranes (*1*, *2*). However, how folding pathways are affected by chaperones remains poorly understood. For instance, it is unclear which steps of the folding process are affected by chaperones, whether the protein-chaperone structure is stable and well defined, and whether native or alternative tertiary interactions are formed in the presence of chaperones.

We addressed these questions by using optical tweezers to induce the mechanical unfolding and refolding of a single protein molecule in the absence and the presence of molecular chaperones. Single-molecule techniques can reveal folding transitions, as has been shown for isolated molecules (*3*–*7*), although they cannot directly correlate the transitions with molecular-level changes in protein structure. To obtain structural insights into the chaperone-free folding pathway, we combined all-atom molecular dynamics (MD) simulations with optical tweezers measurements.

We studied the unfolding and folding of *Escherichia coli* maltose binding protein (MBP) and its dependence on the chaperone SecB (*8*, *9*). The interaction between SecB and MBP has been extensively studied by bulk biochemical assays, making it an ideal system for exploration at the single-molecule level. The known physiological effects of SecB are to reduce aggregation (*10*), to promote translocation across membranes (*11*), and to delay formation of the native state (*12*, *13*). SecB binds to hydrophobic peptide regions (*14*, *15*) and does not require a signal sequence for interaction (*16*). Although the structure of MBP in complex with SecB is unknown, it has been suggested that MBP forms tertiary structure elements in the presence of SecB (*17*). Such elements would need to be disrupted during translocation because only an extended chain can pass through the narrow SecYEG channel (*18*).

Individual MBP molecules were tethered between two polystyrene spheres ~2 μm in diameter by using a 2553–base pair DNA molecular spacer to prevent undesired bead-bead interactions (Fig. 1A). Connections to the N- and C-terminal ends of wild-type MBP were obtained via an engineered biotin group and a quadruple c-myc tag, respectively. Purified constructs, here referred to as MBP, retained their ability to bind to an amylose resin, indicating proper folding. The DNA-protein tether was stretched by displacement of the pipette bead, and the resulting force on the second bead trapped in the laser focus was measured. These experiments yielded force-extension curves (Fig. 1B) showing a sudden change in extension at an average applied force of 25 ± 8 (SD) pN. When MBP was replaced with a plain biotinylated c-myc tag, there were no sudden extension changes (fig. S1), showing that they correspond to MBP unfolding events. After the unfolded MBP was relaxed by moving the beads together, it folded back to its native state, as evidenced by a second stretching experiment that yielded a similar curve. This unfold-refold cycle was reproducible several times on a single molecule until a linkage in the tether broke.

Stretching curves of a second construct composed of four tandem MBP repeats (4MBP) reproduced the unfolding at an average force of 23 ± 4 pN (Fig. 2, A and B). As previously reported for atomic-force microscopy experiments on proteins with repeated domains (*3*, *6*), a saw-tooth pattern was observed, corresponding to the separate unfolding events of the repeats. Interestingly, however, after the force had been lowered to allow refolding, in the second stretching curve the protein often failed to unfold at the normal 25 pN

[1]Department of Molecular Microbiology, Groningen Biomolecular Sciences and Biotechnology Institute and the Zernike Institute for Advanced Materials, University of Groningen, Kerklaan 30, 9751 NN Haren, Netherlands. [2]FOM Institute for Atomic and Molecular Physics (AMOLF), Kruislaan 407, 1098 SJ Amsterdam, Netherlands.

*These authors contributed equally to this work.
†Present address: Philips Research, High Tech Campus 36, 5656 AE Eindhoven, Netherlands.
‡Present address: Laboratoire de Symbiosis Tropicales et Méditerranéennes TA A-82/J, Campus International de Baillarguet, 34398 Montpellier cedex 5, France.
§Present address: McKinsey and Company, Amstel 344, 1017 AS Amsterdam, Netherlands.
‖To whom correspondence should be addressed. E-mail: tans@amolf.nl